



**CHALMERS**  
UNIVERSITY OF TECHNOLOGY

## **Control strategies for refiners Part II: Consistency control in twin-disc refining zones using temperature profile information**

Downloaded from: <https://research.chalmers.se>, 2021-08-31 13:15 UTC

Citation for the original published paper (version of record):

Karlström, A., Hill, J. (2018)

Control strategies for refiners Part II: Consistency control in twin-disc refining zones using temperature profile information

Nordic Pulp and Paper Research Journal, 33(1): 44-57

<http://dx.doi.org/10.1515/npprj-2018-3008>

N.B. When citing this work, cite the original published paper.

## Mechanical pulping

Anders Karlström\* and Jan Hill

# Control strategies for refiners Part II: Consistency control in twin-disc refining zones using temperature profile information

<https://doi.org/10.1515/npprj-2018-3008>

Received August 9, 2017; accepted December 11, 2017; previously published online February 27, 2018 on [www.npprj.se](http://www.npprj.se)

**Abstract:** Consistency profiles in the refining zones of twin-disc refiners have always been cumbersome to estimate with good accuracy. To overcome such challenges, this paper shows that it is vital to measure temperature profiles between the refining discs to estimate uneven chip/pulp feed distribution. It is also shown that the plate clearance, measured by plate gap measurement devices, is changed dramatically when changing the amount of dilution water to the refining zones asymmetrically. At the same time, the inlet temperature will change as well while the maximum temperature is rather stable. This makes the maximum temperature a good candidate for use when estimating the split of the pulp mass flow rates to the refining zones. This also opens for a new consistency control concept for each refining zone. The findings in this paper have been validated in a commercial TMP production line with two serially linked twin-disc refiners, and it is shown that the pulp and handsheet property variations, in terms of mean fiber length and tensile index, between the refining zones can be reduced considerably when running the refiners with similar consistency in each refining zone.

**Keywords:** consistency; modeling; pulp and paper industry; temperature.

## Introduction

The concept of twin-refiner has a history that dates back to the transition period from RMP to thermo-mechanical pulp (TMP) in the 1970's. From a mechanical point of view, the two refining zones in parallel are appealing as there is no need for a heavy-duty axial thrust bearing. On both single and double disc refiners, the axial thrust bearing

has to carry the full load of the refining force. The advantage of being able to design large refiners was pointed out by Carty (1977), although his main concern was the control of the two refining zones. This topic was further elaborated by Vespa et al. (1979). Interestingly, considering the topic addressed in this paper, Vespa et al. implemented individual controls of production rate and consistency of the drive end and tail end gaps. There are some 16 papers that were presented at International Mechanical Pulping Conferences from 1983 until 2001 that deal with twin refiners but, surprisingly, none reverts to the matter of equal refining conditions in the two parallel refining zones.

The Hylte mill installed two lines of two stage twin refiners in 1984. The process and some results were presented by Ulander (1985). It is noticeable that the early design with two chip metering belts or screws from the pre-heater has been replaced by another device usually referred to as a stream splitter. The function of the stream splitter has been described by Mosbye et al. (2001), Eriksen (2003), including some comments on its controllability. There are no publicly reported evaluations of the stream splitter performance. In summary, hardly anything has been published on the production rates and the consistencies in the drive end and tail end since the twin refiner was introduced to the market.

From 1975 (Leask 1975) until 2001, Pulp and Paper Canada published an annual review of TMP installations. These reviews were authored by Ray Leask until 1992 and then by Adrian Barnet. The accumulated number of twin refiners installed in TMP production lines is more than 150, of which about 60 % are still in operation.

Considering the long-term mill observations of unequal conditions of the drive end and tail end gaps, this topic appears to be as important as in the early installations. This situation has recently been even more pronounced due to the reduced demand for newsprint products and increased energy cost. Thus, to stay on the market, it has been necessary for modern mills with TMP processes to focus on reduction of operating costs while maintaining product quality. Minimization of deviations from

---

\*Corresponding author: Anders Karlström, Chalmers University of Technology, Göteborg, Sweden, e-mail: [anderska@chalmers.se](mailto:anderska@chalmers.se)  
Jan Hill, QualTech AB, Tyringe, Sweden, e-mail: [jan.hill@qtab.se](mailto:jan.hill@qtab.se)

target product quality can therefore be considered essential. However, there lies an inherent difficulty in optimizing product quality as there exist many ways to approach the “right” quality. Moreover, due to the complexity of the process, it is difficult to estimate the economic value of reduced variations in pulp properties, see Sikter (2007).

Earlier research has shown that information about temperature profiles, directly measured in the refining zones, can play a vital role in describing the process conditions, see e. g. Mosbye et al. (2001), Johansson (2001), Backlund (2004), Berg et al. (2003), Karlström et al. (2005), Karlström et al. (2008), Eriksson and Karlström (2009), Karlström and Hill (2014a, 2014b, 2015a), Karlström et al. (2015b). Such measurements capture fast dynamics related to the energy balance, which is a necessary piece of information for understanding the cause of variations in pulp properties in a short time scale.

Temperature measurements and plate gap clearance have proven to be robust enough for such extreme process environments. For TMP refining processes, it is an understatement that the robustness of sensors is one of the keys to a successful implementation of reliable control systems and, to meet pulp quality demands, robust control strategies for refiners have been developed where operators face the complexity of the refining processes from a new perspective.

The first section of this paper comprises the fundamental assumptions in estimating the motor load split between the refining zones and the pulp content in each zone. In this section, the assumptions and use of the maximum temperature in each refining zone will be a backbone to get reliable estimations of the backward and forward flowing steam. The next section covers an analysis of the balance between the mass flows, including a comparison of the measured and estimated consistency in the blow-line. In this respect, this paper presents one way to use soft sensors (estimated physical variables) in future on-line control applications. The hypothesis is that a consistency deviation between the FS and DS is not a favorable situation from a process stability and a pulp property development perspective. Therefore, the focus will be on analyzing if it is possible to control the consistency individually on each side by manipulating the dilution water feed rate.

## Materials and methods

The flow pattern in a twin refiner is complex, with three physical internal states (chips, water and vapor) to han-

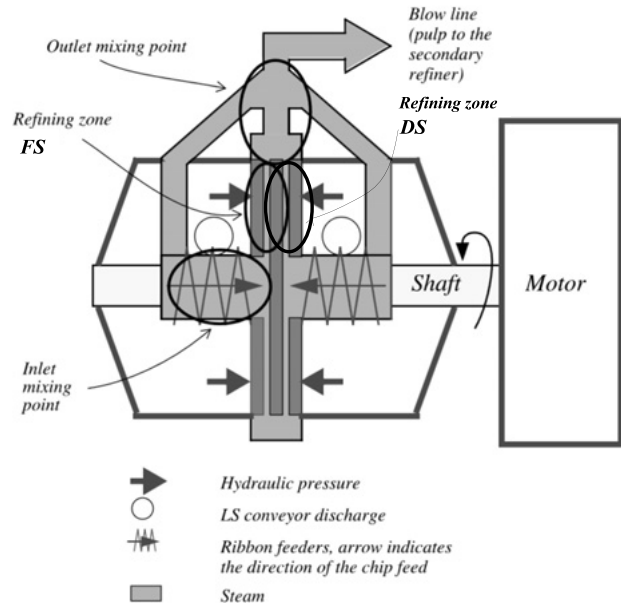


**Figure 1:** Schematic description of a twin-disc refiner. The defibration/fibrillation is performed in two refining zones divided by a rotor. The casing (outlet) is interconnected with the inlet mixing point in the primary refiner to even out the steam pressure and stabilize the feeding system.

dle in two refining zones’ tail end and drive end. Here we prefer to call the refining zones front side – FS – and drive side – DS – as seen in Figure 1. The chips are introduced to the inlet mixing zones by two ribbon feeders, which makes it difficult to predict the feed rate to each zone. The dilution water added to the inlet mixing point is expected to be evaporated in the refining zones. Some of the water bound to the fibers is also vaporized during the defibration and fibrillation of the pulp. The magnitude is difficult to foresee without measuring the temperature profiles and using different modeling techniques.

To overcome some of the problems, Karlström and Eriksson (2014a) introduced a physical model called the “extended entropy model” where the concept of internal variables (e. g. temperature, consistency, fiber residence time, backward flowing steam and forces acting upon the chips and pulp besides traditional external variables, e. g. dilution water feed rate, specific energy and plate clearance) was introduced. The internal variables can be seen as soft sensors useful in future control applications. They differ from the external variables, which are not available as distributed variables from refining zone measurements.

In the extended entropy model, both temperature profiles are included as model inputs. If the plate gap mea-

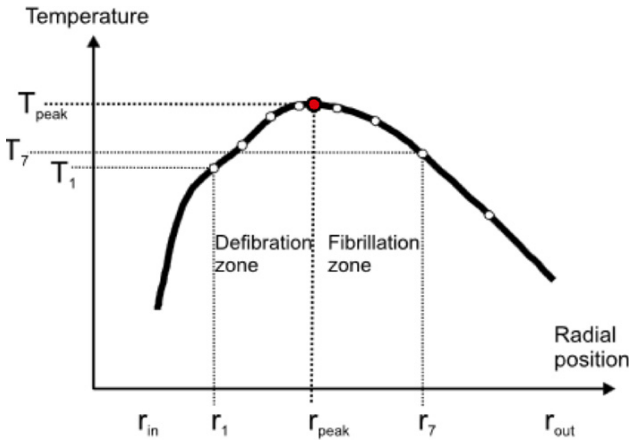


**Figure 2:** A typical temperature profile with the stagnation point indicated at radius  $r_{peak}$  in the refining zones.  $T_1$  indicates the first sensor and  $T_7$  the 7<sup>th</sup> sensor. In this paper the sensor positions  $\approx [30, 55, 80, 100, 125, 160, 175, 205]$  mm along the refining segment.

measurements are available they become inputs as well.<sup>1</sup> In this model, the steam generated in the refining zones is considered to be saturated.

The steam is evacuated both forward (towards the periphery of the segments) and backward (towards the inlet mixing zone) with a stagnation point at some radius in between, see Figure 2.

The stagnation point in Figure 2 coincides with the maximum temperature (or pressure) and implies a zero pressure gradient,  $\partial p/\partial r = 0$ . When modeling the process, it is important to estimate this position,  $r_{peak}$ , (which is also called  $r_{max}$  as it corresponds to the maximum temperature) as it is directly related to the backward and forward flowing steam. Moreover, the position of the zero pressure gradient also affects the pulp velocity and thus how the pulp is developed along the radius of the refining zone.

In this paper, the extended entropy model, derived by Karlström and Eriksson (2014a), has been modified to handle the uneven feed distribution between FS and DS. Both the primary and secondary refiners will be in focus.

As seen in Figure 3, with a schematic illustration of the material and energy balances, two major blocks are included for each refiner model. In the upper figure, the motor load ( $W$ ), plate gaps ( $\Delta$ ), mixing of chips or pulp ( $m_1$ ), steam ( $m_3$ ) and water added<sup>2</sup> ( $D$ ) are introduced as prime

<sup>1</sup> According to Figure 1, the hydraulic pressures are shown as inputs instead of the disc clearances. However, when measuring the distance between the refining segments, the hydraulic pressure can be ignored.

<sup>2</sup> The total water added includes sealing water and dilution water. Internal water flows are denoted as  $m_2$ .

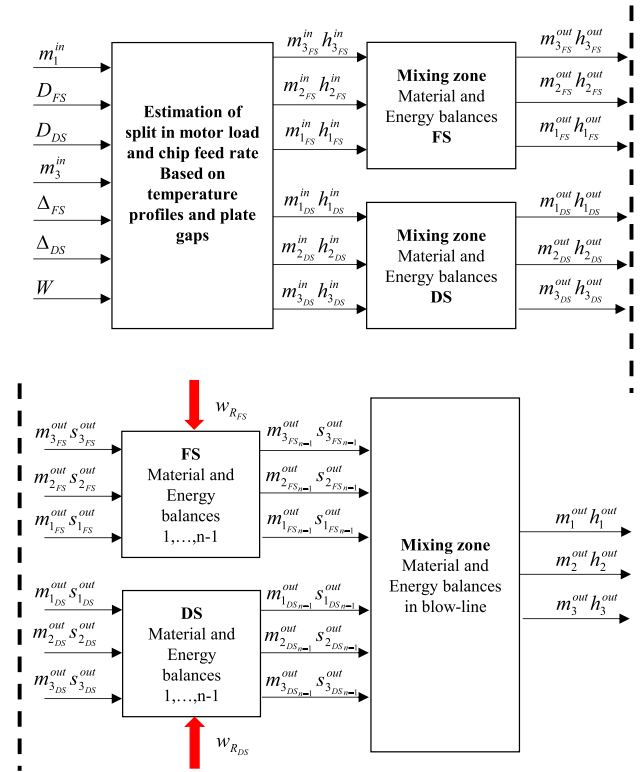


**Figure 3:** Schematic illustration of the material and energy balances for each twin-refiner. The mass flows are represented by  $m$ . Variables  $h$  and  $s$  represent the enthalpy and entropy, respectively. This illustration comprises the concept of soft sensor used in this paper.

inputs to the first block. The models in this block are based on an enthalpy approach where the direction of the steam flow is dependent on actual process conditions in a hypothetical mixing point.

The direction of the steam flow is primarily set by an iterative routine using the entropy model, illustrated by the left blocks in the lower figure in Figure 3.

When modeling twin refiners, the complexity increases as the inlet and outlet are interconnected in the primary refiner, as illustrated in Figure 1, while the secondary refiner is interconnected with the primary stage cyclones. All this makes it difficult to foresee the steam direction beforehand without modeling the system. Hence, the complete model comprises two blocks for motor split estimation and six mixing blocks defined by material and enthalpy balances. In addition, each refiner has two blocks to define the material and entropy balances in the refining zones. In total, the complete system, for two serially linked twin refiners, comprises 12 sub-models which can be used for consistency profile ( $C$ ) estimation.

Consider the process input vector,  $u = [P, \Delta, D]$ , which consists of the elements of production, i. e. wood chip feed

rate ( $P$ ), plate gap for closing the refining zone ( $\Delta$ ) and dilution water feed rate ( $D$ ).<sup>3</sup>

The production is, of course, the same in both primary and secondary refiners while the plate gaps and dilution water added are individual for each zone and therefore divided according to  $[\Delta_{FS}, D_{FS}]$  and  $[\Delta_{DS}, D_{DS}]$ , respectively.

If the internal variables are not available for control, which is the most common situation in the pulp and paper industry, the system description using the specific energy becomes complex (i. e. the ratio of the motor load to the production rate<sup>4</sup>). However, by using internal variables instead, a more sophisticated control concept can be formulated see Karlström and Hill (2018a).

By introducing the pulp quality,  $Q$ , a simple form of the output vector,  $y$ , is obtained at the same time as the system complexity can be reduced considerably due to natural decoupling phenomena, see Karlström and Hill (2018a).

$$y = \begin{bmatrix} T_{\max FS} \\ C_{\max FS} \\ T_{\max DS} \\ C_{\max DS} \\ Q \end{bmatrix} = Gu = \begin{bmatrix} g_{11} & & & & g_{15} \\ & g_{22} & & & g_{25} \\ & & g_{33} & & g_{35} \\ & & & g_{44} & g_{45} \\ g_{51} & g_{52} & g_{53} & g_{54} & g_{55} \end{bmatrix} \begin{bmatrix} \Delta_{FS} \\ D_{FS} \\ \Delta_{DS} \\ D_{DS} \\ P \end{bmatrix} \quad (1)$$

where  $G$  is the transfer function matrix describing the process dynamics. This is a typical MIMO structure where the elements in  $G$  are time varying and difficult to derive.

It is important to note that  $C_{\max FS}$  and  $C_{\max DS}$  always correspond to the periphery positions in the refining zones, i. e. they do not coincide with the positions obtained for the temperature maxima.

Hence, in total, we have a sparse  $5 \times 5$  system<sup>5</sup> to handle for each Twin refiner but, normally, the aim is to

<sup>3</sup> When the plate gap is not available, the input vector become  $u = [PhD]$  where  $h$  corresponds to the hydraulic pressure.

<sup>4</sup> The motor load is normally seen as an output while the production rate, i. e. the chip feed rate to the refiner line, is an input. Therefore, from a control engineering perspective, the specific energy control concept is questionable.

<sup>5</sup> Note that the matrix includes the pulp quality only to give the reader information about the fact that it is affected by all process inputs. Moreover, the pulp quality must be described by several pulp or handsheet properties but normally only a few of these are the prime candidates in control concepts, see Karlström and Hill (2017a, 2017b, 2017c).

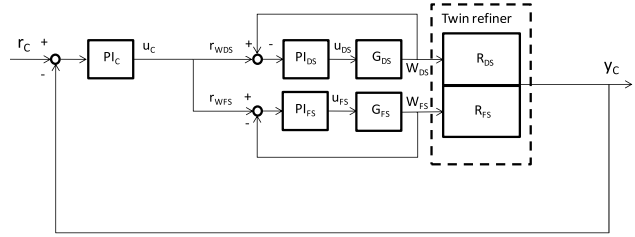


**Figure 4:** Cascaded consistency control loop for a twin refiner. The inner loop controls the dilution water flow rate to the two refining zones that are called FS and DS, respectively.

keep the production as stable as possible which means that we can reduce the system complexity for two serially linked refiners ( $i$ ) even further see Equation 2. The reason is that any disturbance in production is captured by the temperature profile measurements and other internal variables such as consistencies, see Karlström and Hill (2014a, 2014b, 2015a), Karlström et al. (2015b), Karlström and Hill (2018a).

$$y_i = \begin{bmatrix} T_{\max FS_i} \\ C_{\max FS_i} \\ T_{\max DS_i} \\ C_{\max DS_i} \end{bmatrix} = Gu = \begin{bmatrix} g_{11_i} & & & \\ & g_{22_i} & & \\ & & g_{33_i} & \\ & & & g_{44_i} \end{bmatrix} \begin{bmatrix} \Delta_{FS_i} \\ D_{FS_i} \\ \Delta_{DS_i} \\ D_{DS_i} \end{bmatrix} \quad i = \{1, 2\} \quad (2)$$

It is worth mentioning that for secondary refiners the relationship between the consistency changes in the primary refiner and the consistency changes in the secondary refiner is not represented in Equation 2. However, as the consistencies can be estimated by the physical model instantly it is possible to get both  $C_{\max FS2}$  and  $C_{\max DS2}$  also in the secondary refiner every sample.<sup>6</sup>

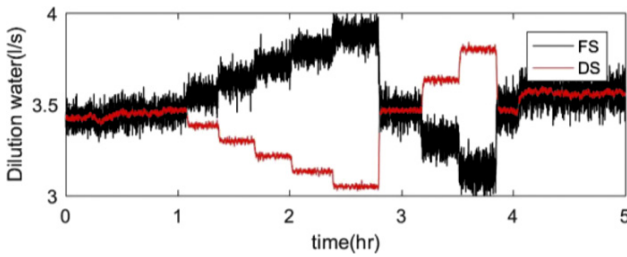
The consistency control loop, illustrated in Figure 4 and Table 1, is based on a traditional cascade control concept for refiners where the dilution water flow rate is controlled (equal mass flow to each refining zone) in the inner loop.

The block called “Twin refiner” in Figure 4 can be seen as the soft sensors providing information about the consistency profiles in FS and DS for the primary and secondary refiners simultaneously. The reason why consistency control in each refining zone is important is that a variable

<sup>6</sup> This opens for an introduction of simple feed-forward loops which modify the dilution water feed rates in the secondary refiner if needed.

**Table 1:** Description of notations used in Figure 4.

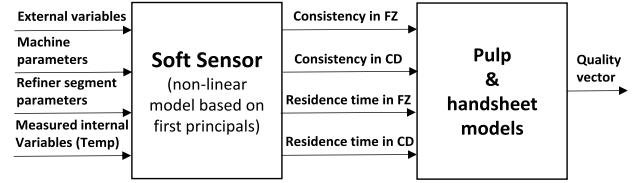
	Description
$r_C$	Reference outer loop, consistency variable.
$y_C$	Output signal; the outer loop, measured consistency.
$W_{DS}, W_{FS}$	Dilution water to the refining zones, DS and FS respectively.
$r_{WDS}, r_{WFS}$	Reference for the dilution water set points on DS and FS.
$u_C$	Dilution water change to adjust the control error, in the outer loop.
$u_{DS}, u_{PS}$	Dilution water change to adjust the control error, in the inner loop.
$PI_C$	Controller for the outer loop, consistency.
$PI_{DS}, PI_{FS}$	Controller for the inner loop (Dilution water control)
$R_{DS}, R_{FS}$	The refining zones

**Figure 5:** Test procedure where the dilution water feed rates are changed symmetrically in opposite directions.

consistency can have a considerable effect on the fiber development see Karlström and Hill (2014a).

The test procedure can be performed in many ways but primarily we will split the dilution water feed rates to FS and DS in opposite directions, as indicated in Figure 5, maintaining the production as stable as possible. The plate gap is not supposed to be controlled during this type of test, which will be discussed in the next section. Other process changes will be commented as well to introduce the reader to typical process responses in Twin refiners.

To check how much better an individual consistency control concept will be regarding improvements in the final pulp and handsheet properties the procedure outlined by Karlström et al. (2015, 2016a, 2016b), Karlström and Hill (2017b, 2017c) will be used. They proposed that the internal variables should be used as predictors when formulating linear estimations of pulp and handsheet properties. In short, it was shown that the consistencies and fiber residence times, according to Figure 6, turned out to be especially essential when estimating pulp and handsheet prop-

**Figure 6:** Schematic description of the soft sensor and the regression model for pulp and handsheet property estimation.

erties using linear modeling techniques.<sup>7</sup> To illustrate the concept, we have implemented this technique for mean fiber length and tensile index estimation using the soft sensors – consistency and fiber residence time.

## Results and discussion

The main topic of this paper is to estimate the consistency in the two zones of a twin refiner. With knowledge of the steam and water mass flows based on the material and energy balances, the entire consistency profile can be derived using the model structure in Figure 3. However, here, we focus on the estimated outlet consistencies from each refining zone and the estimated weighted blow-line consistency, which is verified using a measured blow-line consistency.

Estimation of mass flow ratio based on plate gap measurements: If the plate gaps are measured properly, it is possible to approach the problem of an uneven feed distribution to the refining zones if the dilution water feed rates to each refining zone are equal.

Assume that the hydraulic pressures on each stator holder are almost equal independent of the refining zone studied.

If the added dilution water feed rates in the twin refiner are equal on each side, it is assumed that the fiber mass flow distribution,  $m_1$ , can be derived using the plate gap measurements  $\Delta$ .

$$m_{1_{FS}} / (m_{1_{FS}} + m_{1_{DS}}) \approx \Delta_{FS} / (\Delta_{FS} + \Delta_{DS}) \quad (3)$$

The plate gaps are seldom equal, and one reason is that most often  $m_{1_{FS}} \neq m_{1_{DS}}$ . As the difference in dilution water feed rates to each zone is normally negligible, as is the difference in hydraulic pressures on the static holders, it is natural to assume that the same situation occurs

<sup>7</sup> The complete concept of pulp and handsheet property estimation is described in more details in Karlström and Hill (2017a, 2017b, 2017c), Karlström and Hill (2018a).

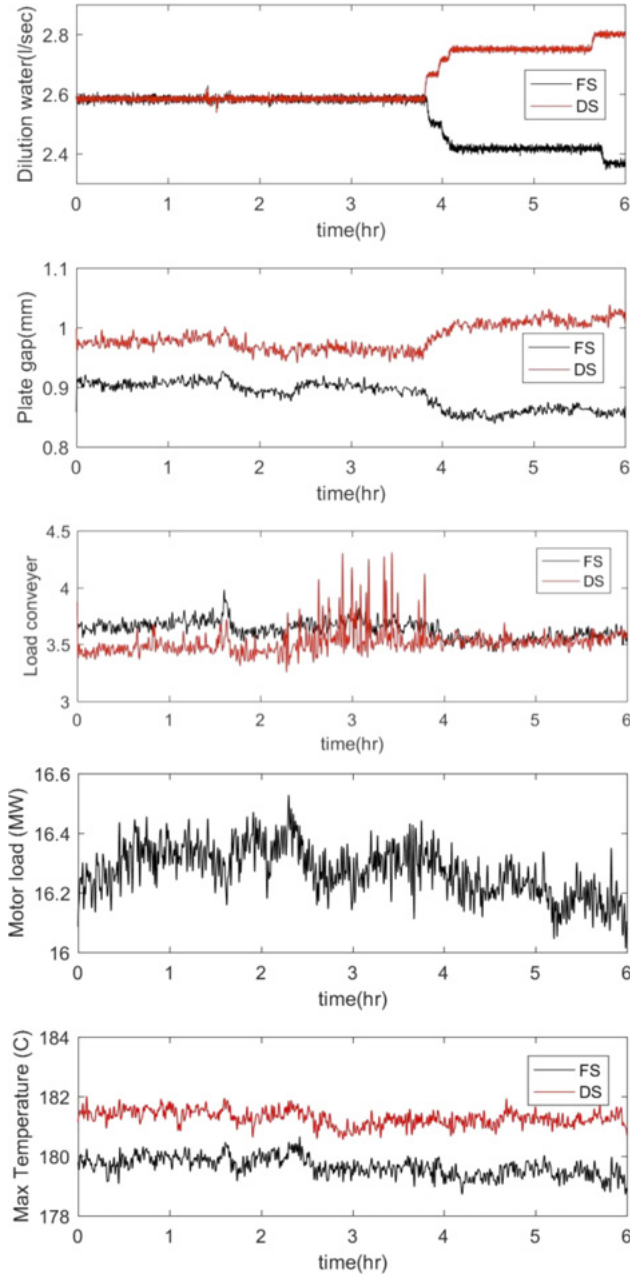


**Figure 7:** Upper figure: Dilution water feed rates to each refining zone. Middle figures: Plate gaps, load conveyor effects and motor load response. Lower figure: Maximum temperatures.

when feeding the refining zones with chips and fibers, i. e.  $m_{1_{FS}} > m_{1_{DS}}$  if  $\Delta_{FS} > \Delta_{DS}$ .

Consider a case, for a primary twin refiner, where the mass flow of chips to each side is not changed while the dilution water is changed in the opposite direction, see Figure 7.

Neither production nor the hydraulic pressure is changed during the test described in Figure 7. The split in water feed rates will affect the vapor balance and thereby

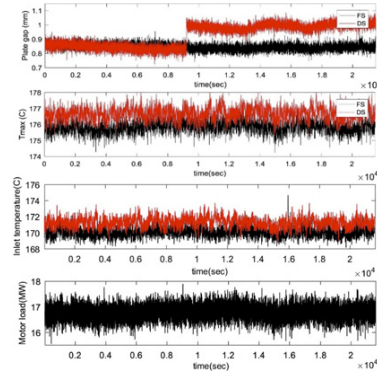


**Figure 8:** Plate gap calibration, lower figures: Process conditions.

cause a change in the plate gaps. When using the ratio specified in Equation 3, the consequence will be that unrealistic chip mass flows on FS and DS are estimated. In Figure 7, neither the load conveyor effects nor the motor load are changed, as expected. As reported in earlier papers, see Karlström and Hill (2014a), the maximum temperature is not expected to be modified very much when the dilution water feed rates are changed, which is also verified in Figure 7. Thus, when the dilution water feed rates to FS and DS differ from each other, the assumption in Equation 3 no longer holds.

Another problem related to plate gap measurements is that we cannot guarantee that the plate gap can be measured with good accuracy. This is best illustrated by studying the on-line calibration of the plate gap sensors<sup>8</sup> in Figure 8. Both sensors are calibrated at the same time, but the distance in DS (and not FS) will be modified even though the process is stable. In this example, the split in mass flow between the refining zones will be wrong if Equation 3 is used. Such issues are normally not a problem when the plate gaps are changed in the same direction, see Figure 9, as the split in mass flows according to Equation 3 will not be changed. Still, we do not know if the measurements are right in this case as both sensors are measuring a distance below 0.5 mm, which of course is questionable. Nevertheless, it is also interesting to see that Figure 9 covers a conscious change in hydraulic pressure (plate gap). The change results in a clear response in the inlet and maximum temperatures, and this information<sup>9</sup> can be used to estimate the motor split between FS and DS.

<sup>8</sup> The gap sensors are manufactured by Dametric AB. The calibration is performed automatically by moving the tip of the sensor towards the rotor segment. This calibration procedure is performed during production.

<sup>9</sup> Note that  $T_{\max FS} > T_{\max DS}$  while  $T_{in FS} < T_{in DS}$ .



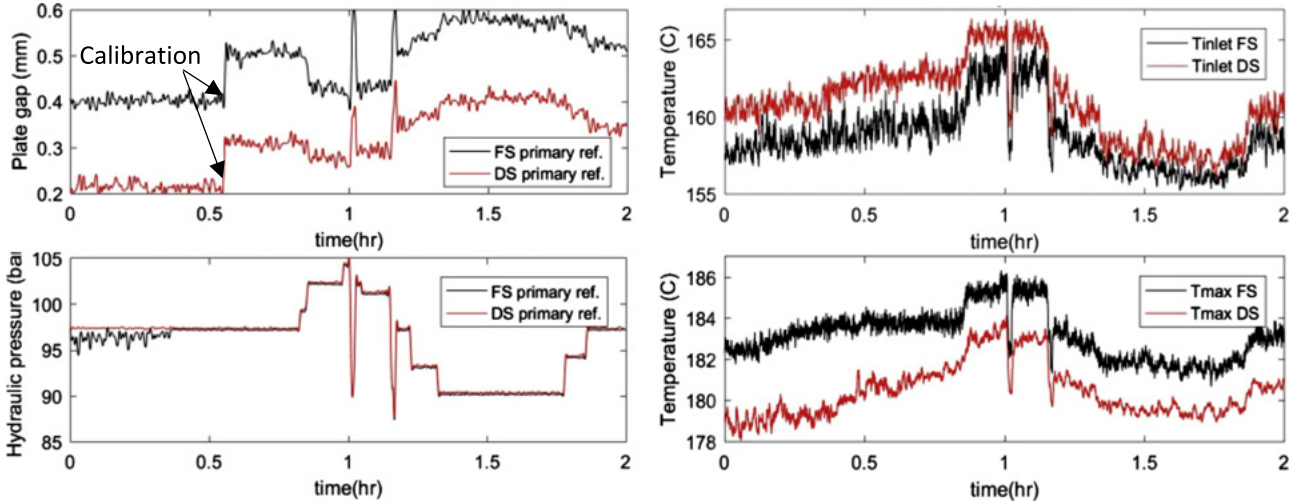


Figure 9: Plate gap calibration and conscious change in plate gap.

It is well known that the temperature profile is affected by changes in the plate gaps according to Figure 9 as is the fact that production and dilution water feed rate changes affect the temperature profile. In principle, increased production affects the temperature profile in the same way as a reduced plate gap.

Estimation of mass flow ratio based on maximum temperature measurements: Production is kept as stable as possible during normal process conditions, which means that it is relevant to study changes in the dilution water feed rates in more detail.

It is interesting to see that the inlet temperatures in both the primary and secondary refiners are affected while the maximum temperature, at least in the secondary refiner, is rather stable, see Figure 10.

It is also interesting to note that the differences in the maximum temperatures between each side are considerable.

The entire temperature profile should be analyzed to fully understand the dynamics related to variations in the steam balance in the refining zones. However, at this stage, it is accepted that all information necessary to derive the consistency profiles in the refining zones is not covered.

As concluded above, the maximum temperature follows the plate gap quite well. At the same time, it is almost unaffected when the dilution water fed to each zone in a twin refiner is manipulated, and this can be used to derive the ratio between the pulp mass flows in Equation 3.

Introduce the following relations:

$$\left. \begin{array}{l} T_{\max_{FS}} < T_{\max_{av}} \\ T_{\max_{DS}} > T_{\max_{av}} \end{array} \right\} \rightarrow \delta_{FS} > \delta_{DS} \rightarrow \delta_x \approx \delta - (T_{\max_x} - T_{\max_{av}})k \quad (4)$$

In this context,  $\delta$ , which is a fictitious distance between the segments, can be set to e. g. 1. The constant,  $k$ , can be set within the interval [0.5 0.15]. The subscript  $av$  represents the mean values of  $T_{\max}$  and  $x$  the specific refining zone FS, DS studied. This means that we introduce the following relation between the mass flows and the temperature maximum:

$$m_{1_{FS}} / (m_{1_{FS}} + m_{1_{DS}}) \approx \delta_{FS} / (\delta_{FS} + \delta_{DS}) \quad (5)$$

which is not dependent on the plate gap changes caused by changes in the vapor balance between FS and DS.

Besides having knowledge about the pulp mass flow in each refining zone, it is important to describe the shape of the temperature profile in detail. The reason is that the shape of the profile is dependent on water and steam mass flows as well as the “true” plate gap and other refining parameters. By using the model structure in Figure 3, and the measured or estimated plate gap, it is possible to estimate the defibrating/fibrillation work on each side.

Assume that the estimated total work along the radius is

$$W_x = 2\pi \int_{r_{in}}^{r_{out}} r w_x dr; \quad x = \{FS, DS\} \quad (6)$$

where the distributed work is described by the relation

$$w_x = \mu_x(T) r^2 \omega^2 / \Delta_x(r) \quad (7)$$

and  $\omega$  is a constant representing the angular speed of the refiner disc. Note that vector  $\Delta_x(r)$  corresponds to a distributed distance between the refining segments, i. e. it is dependent on the radius,  $r$ . Thus it is understood that  $W_x = f(T_x(r), \Delta_x(r))$  if the pulp viscosity,  $\mu_x(T)$ , is known.



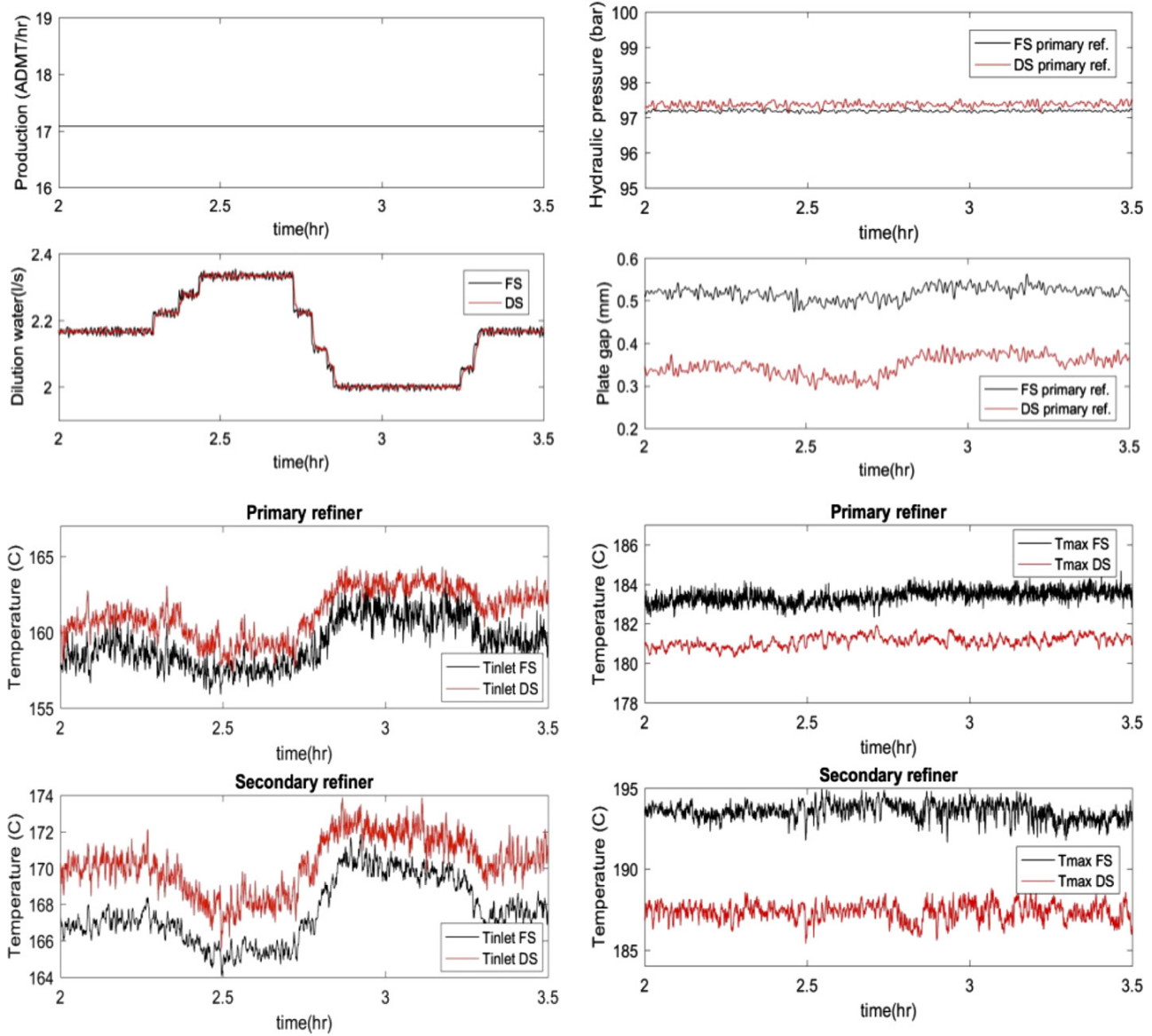


Figure 10: Temperature responses (inlet and maximum) when changing dilution water feed rates to the primary refiner.

The absolute value of  $\mu_x(T)$  is difficult to estimate but, as described by Karlström and Eriksson (2014a, 2014b, 2014c, 2014d), a relatively good approximation can be obtained. However, it is not critical to know the absolute value as the focus is on the relationship between FS and DS, i. e. the ratio  $\mu_{FS}(T)/\mu_{DS}(T)$ .

Moreover, as mentioned in the previous section, it is important to estimate the position  $r_{peak}$  (i. e.  $r_{max}$ ) as it directly relates to the position at which the backward and forward flowing steam is zero. However, when the temperature profile is not available, the inlet steam mass flow rate is impossible to derive. This certainly affects the accuracy of the mass flow estimation of both water and steam. However, assuming that

$$m_{3_x} \approx 0 \text{ at } T_{max_x}; \quad x = \{FS, DS\} \quad (8)$$

it is possible to derive the steam flow to (or from) the inlet of the refining zone using the model structure in Figure 3. It is necessary to cope with all this when estimating final consistency profile in FS and DS. In this paper, we focus only on the outlet consistency from each refining zone.

Suppose that the dilution water feed rates to FS and DS are changed in opposite directions according to Figure 5. This manipulation will affect the plate gap directly as the spatial steam pressure will be changed see Figure 11.

A small asymmetry is obtained for the valve opening, see Figure 12, which most likely is a consequence of differ-

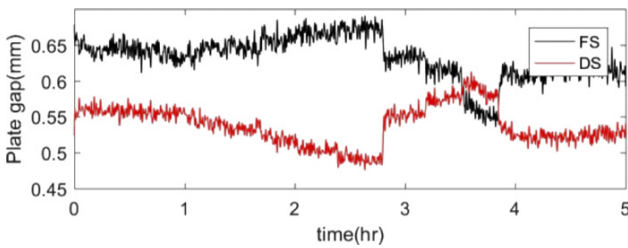


**Figure 11:** Changes in plate gaps when changing dilution water feed rates according to Figure 5.

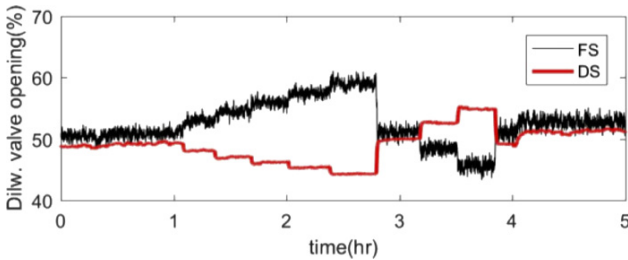
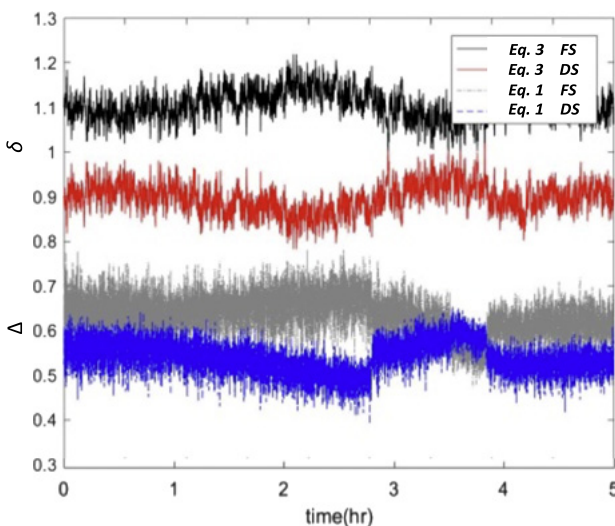


**Figure 12:** Dilution water valve opening according to changes in Figure 5.

ent pulp mass flows and a shift in the steam balance between the refining zones.

To illustrate the consequences when changing from a measured plate gap ratio to a temperature based ratio, it is important to see how the two approaches differ from each other when the dilution water feed rates to each refining zone are similar.



As can be seen in Figure 13, the ratios when using those in Equation 3 and Equation 5 correspond quite well. This is promising as it sometimes is hard to secure the accuracy in the plate gap measurements.

Consistency estimation in twin refiners: The consistency profiles on FS and DS can be derived by applying the model described in Figure 3 to the process data, see further Karlström and Hill (2014a, 2014b). It is of course difficult to validate each consistency, but the “weighted sum” of the estimated consistencies from each side can be compared with the measured consistency in the blow-line.

Following the test procedure outlined in Figure 5 it is easy to see that the estimated and measured consistencies in the blow-line are almost independent of the plate gap, see Figure 14. However, the consistencies in FS and DS are affected considerably due to the change in the dilution water feed rates.

When using the ratio described by Equation 3, the consistencies in FS and DS are changed dramatically (about 10 % in DS) while a more modest change occurs when the plate gap is set as a constant. Note that, when the plate gap is set as a constant, the ratio in Equation 5 is not used. This indicates that the plate gap change affects the consistency in the same direction as the entire temperature profile, which is an unrealistic situation. This also means that the consistency dynamics are indirectly covered by the temperature profile changes, which is partly confirmed in Figure 15, where the inlet temperatures are changed while the maximum temperatures are rather stable.

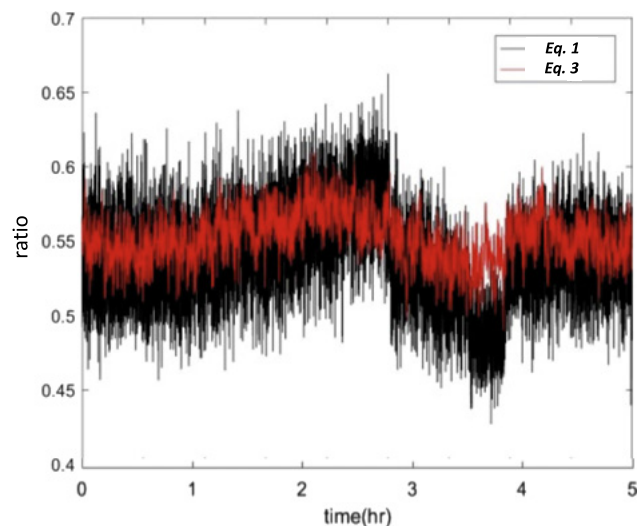


**Figure 13:** Left: Measured (grey and blue) plate gaps and estimated (black and red) temperature relations. Right: Ratio related to mass flows according to Equation 3 and Equation 5. Note that, in this case, the variables are not filtered, which also gives a hint about the disturbances involved when using the different concepts.

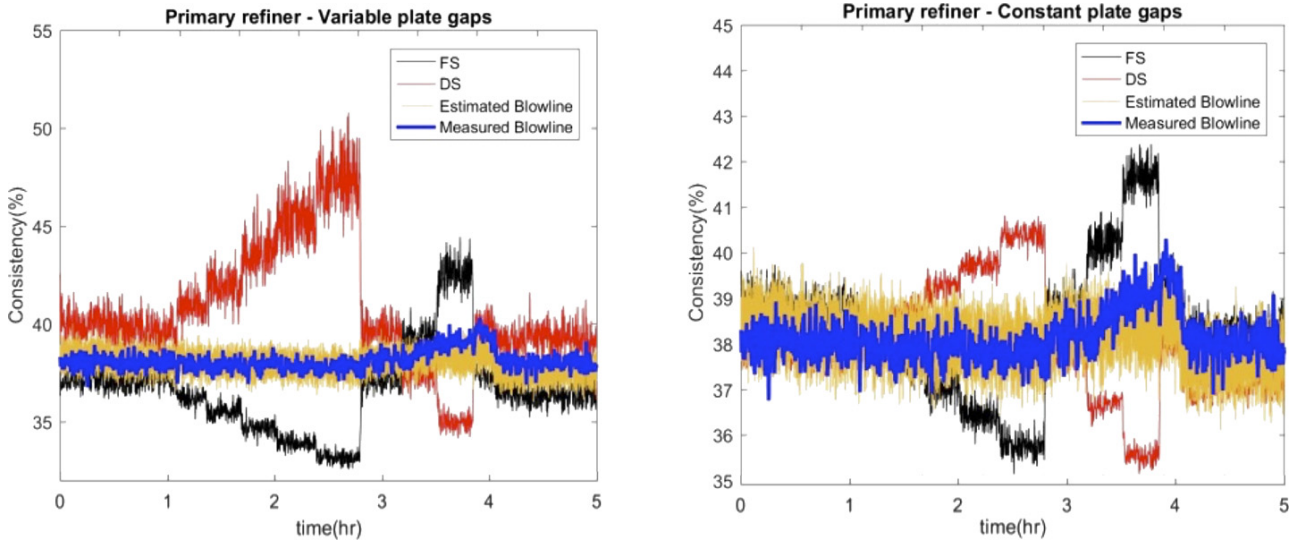


Figure 14: Left: Measured and estimated consistencies in the blow-line, FS and DS. Estimation based on plate gap measures. Right: The same as in the left figure but with an assumed constant plate gap.

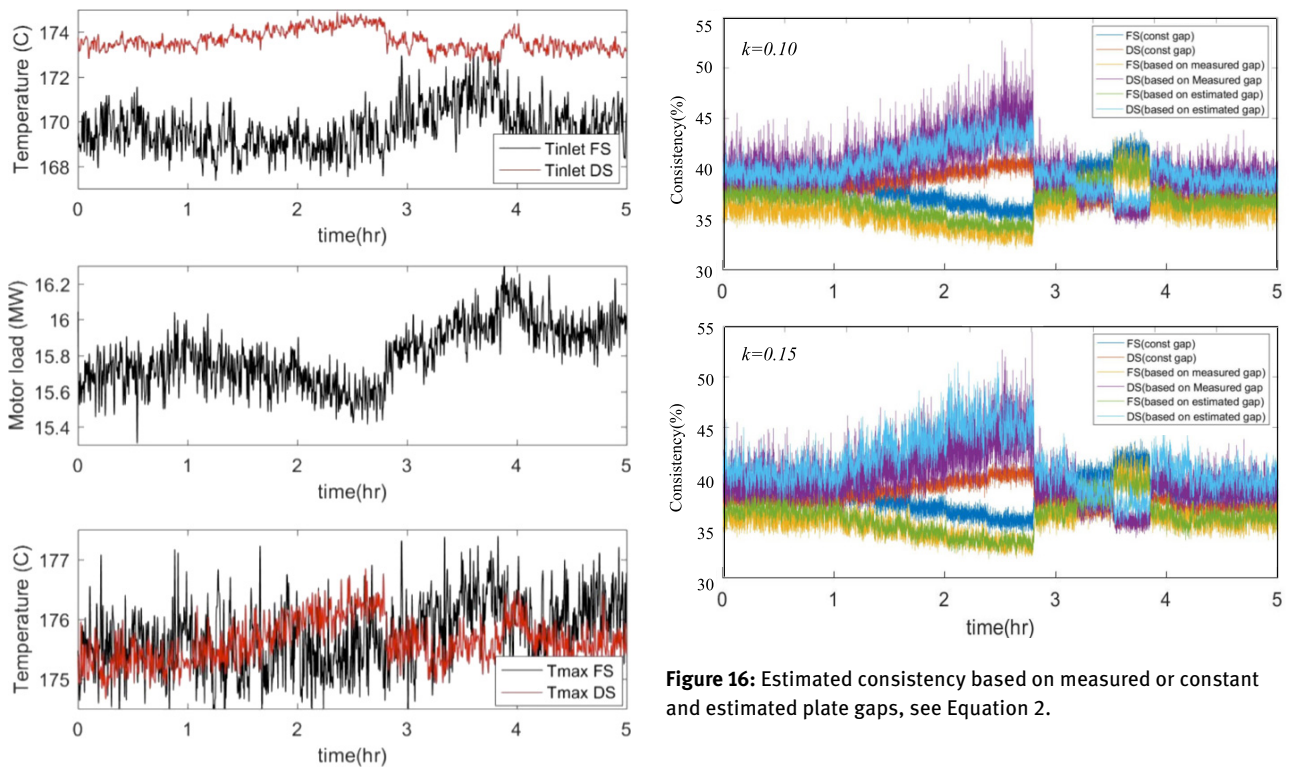


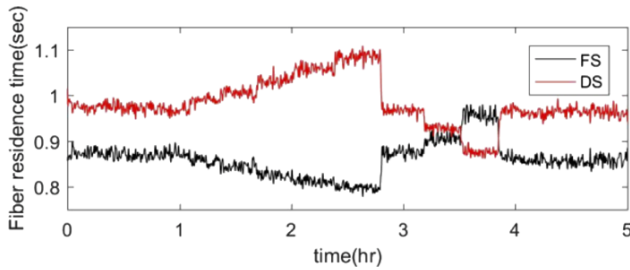
Figure 15: Motor load, inlet and maximum temperature before and after the step changes in dilution water feed rates.

Figure 16: Estimated consistency based on measured or constant and estimated plate gaps, see Equation 2.

It is also interesting to see in Figure 15 that the temperatures in FS are much noisier than those in DS. This is most likely a consequence of the uneven feed distribution, which makes it more difficult for the steam to be evacu-

ated from the refining zone in FS. The reason why the motor load is increased closer to the end of the studied interval can be an effect of a slightly reduced plate gap on each side.

Even though the resolution in the maximum temperatures is normally small the dynamics are sufficient to motivate a deeper study of the relations in Equation 4. As seen in Figure 16 the information obtained illustrates how



**Figure 17:** Estimated fiber residence times in each refining zone when changing the dilution water feed rates.

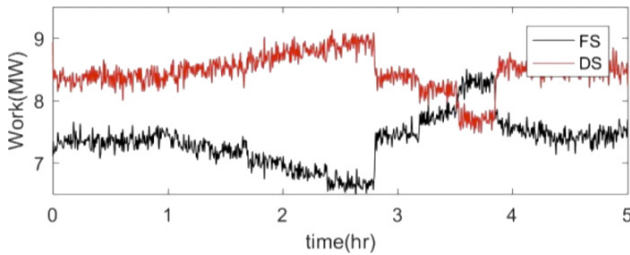


**Figure 18:** Estimated motor load split when changing the dilution water feed rates.

a combined effect of both dilution water feed rate, plate gap and temperature profile changes affects the process conditions; to optimize pulp quality, this is important to cope with in future control applications.

**Fiber residence time and pulp quality:** According to Karlström and Hill (2014a), the fiber residence time in the refining zone can be estimated if the process variables in terms of external and internal variables are known together with refining segment parameters such as e. g. taper, bar and groove widths. In this case, where the twin refiners are in focus, all necessary information is available to estimate the fiber residence time and the motor load split, see Figure 17 and Figure 18.

Assume that the defibration/fibrillation follows a common pattern in all types of refiners, i. e. an increased fiber residence time will lower the mean fiber length and increase the tensile index to a certain operating point regardless of the refining segment used. If this assumption is applicable, the same approach as outlined by Karlström et al. (2015, 2016a, 2016b) can be used when estimating the mean fiber length (*MFL*) and tensile index using a multivariate linear equations, see earlier section or Karlström et al. (2015, 2016a, 2016b), Karlström and Hill (2017b, 2017c).

If we consider the fiber residence time in Figure 17, two different intervals are of specific interest, namely the first samples (time 0–0.3 hr) when the process is running with-

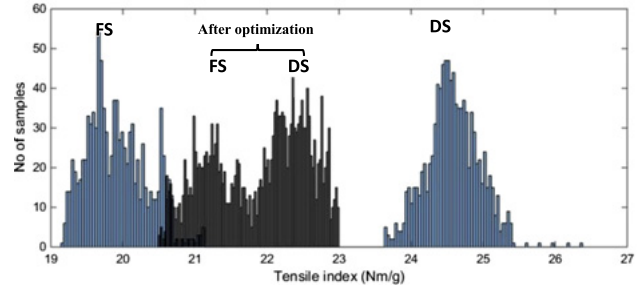
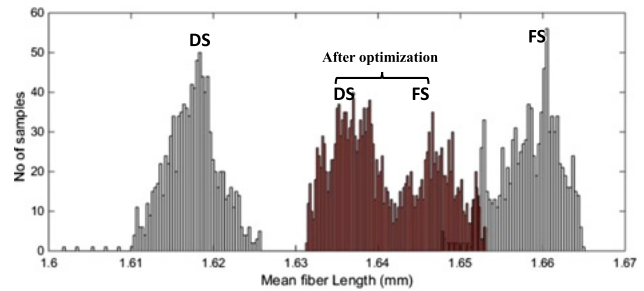


**Figure 19:** Pulp property distribution before and after dilution water optimization based on  $1000 \times 144$  samples from process data. Upper figure; Mean fiber length. Lower figure: Tensile index.

out a change in dilution water split to FS and DS, and when the residence times in Figure 17 converge (time 3.5–3.8 hr). Using the pulp property estimations, it will be possible to optimize the distributions in *MFL* and tensile index, see Figure 19. The magnitude of the improvement can be discussed, but it is clear that a more dense distribution will be obtained.<sup>10</sup>

Further improvements concerning the pulp property distribution will be made in the future by following the methods outlined by Karlström and Hill (2017b, 2017c). The tests in this paper were performed in manual mode for only one refiner and without process control. Implementing the physical model on-line, as described briefly in this paper, will most likely improve the pulp property development even further.

## Conclusions

This paper proposes an extended consistency control scheme in twin refiners by manipulating the dilution water feed rates to each refining zone individually. The analysis

<sup>10</sup> In this specific case,  $MFL \approx -0.4\tau + 2$  and  $TI \approx 46\tau - 20.3$ , where  $\tau$  is the fiber residence time. These simplified models comprise an average of all models with a normal consistency profile in the refining zone. The modeling concepts are well described for a CD82 refiner by Karlström et al. (2015, 2016a, 2016b).



is based on process data from dynamic tests in a commercial production line comprising two serially linked twin refiners. The control concept focuses on the primary refiners but can be extended to cover secondary refiners as well.

In measuring the temperature profiles and the plate clearance between the refining discs, it is concluded that the pulp mass flows in the refining zones can be estimated. It is shown that the maximum temperature in each refining zone can be used for pulp mass flow estimation. This is especially a good choice when different dilution water flow rates are fed to the refining zones. The reason why the plate gap measurements fail to be used in such situations is that the vapor balance affects the plate gap clearance and thereby the possibility to find proper pulp mass flow estimations. Moreover, the extended entropy model can be used to understand how the work is split between the refining zones due to the uneven chip/pulp feed distribution. This together with the fact that the backward and forward flowing steam is negligible at the maximum tem-

peratures makes it possible to derive the steam mass flows in each refining zone.

This paper shows that the consistency in FS and DS can deviate considerably. The difference in consistency between the sides can be as large as 2–4 % when using the maximum temperature ratio, even though the estimated consistency in the blow-line coincides with the measured consistency. It is notable, when the plate gap measurements are used to find a proper ratio between mass flows in FS and DS that the consistency deviations between the zones can approach 10 %, which is certainly not possible. This is a consequence of the fact that temperature profile changes and plate gap changes act in the same direction.

Finally, the pulp property development in terms of mean fiber length and tensile index is discussed. Using a pre-defined relation between the pulp properties and fiber residence time makes it possible to illustrate the expected difference in fiber distribution between the front side and the drive side in the twin refiner. As an example, the esti-

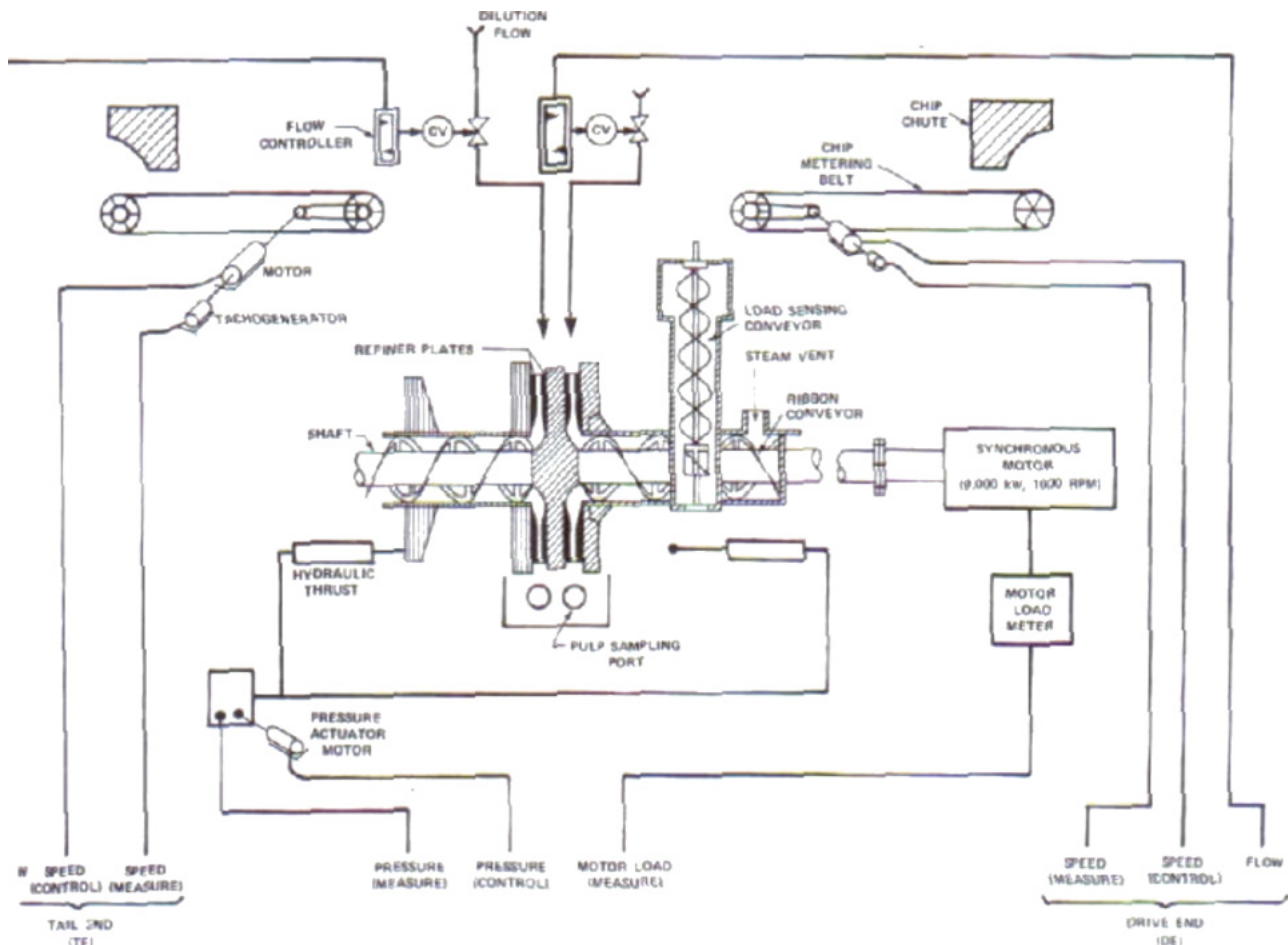


Figure 20: Schematic lay-out of process and instrumentation in the twin TMP line presented by Vespa et al. (1979).

mated tensile index mean difference between the refining zones will be reduced from 4.5 Nm/g to 1.2 Nm/g when optimizing the process.

**Acknowledgments:** Special thanks go to StoraEnso Hylte mill for performing trials and providing the process data used in this study.

**Funding:** The authors gratefully acknowledge the funding by the Swedish Energy Agency.

**Conflict of interest statement:** The authors do not have any conflicts of interest to declare.

## Appendix

Initially, there was considerable concern that the drive end (DE) and tail end (TE) would receive equal production rates. This is demonstrated by the design shown in Figure 20 presented by Vespa et al. (1979). It is worth mentioning that an alternative design was also presented by Carty (1977).

The system developed by Vespa et al. (1979) is described by bloc diagrams for specific energy control and consistency control. Obviously, the feed rates of the two metering belts are controlled individually. The consistency is not controlled individually, however, despite having individual sampling ports of the DE and TE refining zones. Their text does not offer any additional explanation to that end.

Ulander (1985) reports on the installation of two lines of two stages of twin refiners. Here the individual feeds of the chip refiner have been replaced by a stream splitter. The function of the stream splitter was studied by Mosbye et al. (2001). Their study was conducted in the Norske Skog Follum mill on a twin line almost identical in its process design as the one presented by Ulander (1985). The stream splitter in Follum was supplied with an automatic system providing the possibility to change the angular position of the two screws of the steam splitter to each other. Their results show that the split of the production to the DE and TE side can be affected. When the temperature profiles of the two zones are equal, the accelerations are almost equal on the DE and TE sides, which strengthens that the conditions in the two zones are close to equal. The difficulty in maintaining equal production rates and conditions in the DE and TE zones is further reported by Eriksen et al. (2003). When optimized, the coefficient of variation of the primary

stage refiner load decreased to about two thirds of the preceding level. This improvement was also confirmed by a substantial decrease in the refiner vibration. There was no noticeable improvement when the same approach was applied to secondary stage refiners.

## References

- Backlund, H.-O. (2004) "Measurement of shear force, temperature profiles and fibre development in mill-scale TMP refiners", Licentiate Thesis, Mid Sweden University, Sundsvall, Sweden.
- Berg D., Karlström A. and Gustavsson, M. (2003) Deterministic consistency estimation in refining processes. In: Proceedings, Int. Mech. Pulp. Conf., Quebec City, Canada, Quebec, Canada, pp. 361–366.
- Carty, W.D. (1977) Process control-Large horsepower thermal mechanical pulping systems. In: Proceedings, Int. Mech. Pulp. Conf., Helsinki, Finland, pp. 37:1–37:6.
- Eriksson, K., Karlström, A. (2009) Refining Zone Temperature Control: A good choice for Pulp Quality Control? In: Proceedings, Int. Mech. Pulp. Conf., Sundsvall, Sweden, pp. 67–74.
- Eriksen, O., Mosbye, K., Johansson, O., Rice, T., Boyd, C., Gregersen, O., Krogstad, P.-Å., Hammer, E., Muggerud, E. (2003) Diagnosis of a first stage mill-scale TMP refiner by means of refining zone pressure and temperature measurements and blow line pulp analysis. In: Proceedings, Int. Mech. Pulp. Conf., Quebec City, Canada, pp. 389–398.
- Johansson O. (2001) Controlling high consistency refining conditions through refining zone temperature optimisation. In: Proceedings, 6<sup>th</sup> Pira International refining conference, Toronto, Canada.
- Karlström A., Berg D., Eriksson K. (2005) Developments in soft sensors for measurement of refining parameters, Scientific and technical advances in refining and mechanical pulping, Barcelona, Spain, Paper.
- Karlström A., Eriksson K., Sikter D., Gustavsson M. (2008) Refining models for control purposes. Nord. Pulp Pap. Res. J. 23(1):129–138.
- Karlström, A., Eriksson, K. (2014a) Fiber energy efficiency Part I: Extended entropy model. Nord. Pulp Pap. Res. J. 29(2):322–331.
- Karlström, A., Eriksson, K. (2014b) Fiber energy efficiency Part II: Forces acting on the refining bars. Nord. Pulp Pap. Res. J. 29(2):332–343.
- Karlström, A., Eriksson, K. (2014c) Fiber energy efficiency Part III: Modeling of fiber-to-bar interaction. Nord. Pulp Pap. Res. J. 29(3):401–408.
- Karlström, A., Eriksson, K. (2014d) Fiber energy efficiency Part IV: Multi-scale modeling of refining processes. Nord. Pulp Pap. Res. J. 29(3):409–417.
- Karlström, A., Hill J. (2014a) Refiner Optimization and Control Part I: Fiber residence time and major dynamic fluctuations in TMP refining processes. Nord. Pulp Pap. Res. J. 29(4):635–652.
- Karlström, A., Hill J. (2014b) Refiner Optimization and Control Part II: Test procedures for describing dynamics in TMP refining processes. Nord. Pulp Pap. Res. J. 29(4):653–662.



- Karlström, A., Hill J. (2015a) Refiner Optimization and Control Part III: Natural decoupling in TMP refining processes. *Nord. Pulp Pap. Res. J.* 30(3):417–425.
- Karlström, A., Eriksson, K., Hill J. (2015b) Refiner Optimization and Control Part IV: Long term follow up of control performance in TMP processes. *Nord. Pulp Pap. Res. J.* 30(3):426–435.
- Karlström, A., Hill J., Ferritsius, R., Ferritsius, O. (2015): Pulp Property Development Part I: Interlacing Undersampled Pulp Properties and TMP Process Data using Piece-wise Linear Functions. *Nord. Pulp Pap. Res. J.* 30(4):599–608.
- Karlström, A., Hill J., Ferritsius, R., Ferritsius, O. (2016a) Pulp Property Development Part II: Process Nonlinearities and its Influence on Pulp Property Development. *Nord. Pulp Pap. Res. J.* 32(2):287–298.
- Karlström, A., Hill J., Ferritsius, R., Ferritsius, O. (2016b) Pulp Property Development Part III: Fiber Residence Time and Consistency Profile Impact on Specific Energy and Pulp Properties. *Nord. Pulp Pap. Res. J.* 32(2):300–306.
- Karlström A., Hill J. (2017a) CTMP process optimization Part I: Internal and external variables impact on refiner conditions. *Nord. Pulp Pap. Res. J.* 32(1):35–44.
- Karlström A., Hill J. (2017b) CTMP Process Optimization Part II: Reliability in Pulp and Handsheet Measurements. *Nord. Pulp Pap. Res. J.* 32(2):253–264.
- Karlström A., Hill J. (2017c) CTMP Process Optimization Part III: On the Prediction of Scott-Bond, Z-strength and Tensile index. *Nord. Pulp Pap. Res. J.* 32(2):266–279.
- Karlström A., Hill J. (2018a) Control Strategies for Refiners Part I: CTMP Process Optimization. *Nord. Pulp Pap. Res. J.* 33:1.
- Leask, R.A. (1975) A review of thermo-mechanical pulping. *Pulp Paper Canada* 76(10, T294).
- Mosbye K., Kure K.-A., Fuglem G., Johansson O. (2001) Use of refining zone temperature measurements for refiner control. In: *Proceedings, International Mechanical Pulping Conference, Helsinki, Finland*, pp. 481–488.
- Sikter, D. (2007) Quality Control of a Newsprint TMP Refining Process based on Refining Zone Temperature Measurements, Licentiate thesis, Chalmers University of Technology, Göteborg, Sweden.
- Ulander, E. (1985) Double benefit – Economy and Quality – with Twin refiners at Hylte Bruks AB. In: *Proceedings Int. Mech. Pulp. Conf., Stockholm, Sweden*, pp. 120–127.
- Vespa, S.C., Mills, C., Butler, D.J, Legault, N.D., Rogers, J.H. (1979) Automatic control of chip refining. In: *Proceedings, Int. Mech. Pulp. Conf., Toronto, Canada*.